International Journal of Marine Energy 19 (2017) 332–344

Contents lists available at ScienceDirect

International Journal of Marine Energy

journal homepage: www.elsevier.com/locate/ijome

Tidal resource and interactions between multiple channels in the Goto Islands, Japan

S. Waldman [a,*], S. Yamaguchi [b], R. O'Hara Murray [c], D. Woolf [a]

[a] Heriot-Watt University, Back Road, Stromness, Orkney KW16 3AW, UK
[b] Department of Earth System Science and Technology, Kyushu University, Fukuoka, Japan
[c] Marine Scotland Science, Scottish Government, 375 Victoria Road, Aberdeen AB11 9DB, UK

ARTICLE INFO

Article history:
Received 17 March 2017
Revised 6 September 2017
Accepted 19 September 2017
Available online 30 September 2017

Keywords:
FVCOM
Numerical modelling
Goto Islands
Tidal energy
Split channels

ABSTRACT

The Goto Islands in Nagasaki Prefecture, Japan, contain three parallel channels that are suitable for tidal energy development and are the planned location for a tidal energy test centre. Energy extraction is added to a 3D numerical hydrodynamic model of the region, using a sub-grid momentum sink approach, to predict the effects of tidal development.

The available resource with first-generation turbines is estimated at 50–107 MW peak output. Spreading turbine thrust across the whole cross-section to prevent bypass flow results in a 64% increase in peak power in one channel, highlighting the importance of 3D over 2D modelling.

The energy available for extraction in each strait appears to be independent of the level of extraction in other straits. This contrasts with theoretical and numerical studies of other multi-channel systems. The weak interactions found in this study can be traced to the hydraulic effects of energy extraction not extending to neighbouring channels due to their geometry.

1. Introduction

1.1. Background

In 2010 nuclear power provided 25% of Japan's electricity [1], making Japan the third-largest producer of nuclear energy in the world [2]. Following the tsunami of 2011 and the subsequent events at the Fukushima Daiichi nuclear power plant this figure dropped to less than 2% (in 2012) as the nation's reactors were taken off-line, and most of the shortfall was replaced by fossil fuels. Lacking substantial fossil resources of its own, by 2015 Japan had become one of the world's greatest importers of fossil fuels, and in addition to the environmental implications this represents a significant drain on economic resources [2]. While there has been some limited resumption of nuclear generation, this is deeply unpopular with sections of the public [3]. As part of a strategy to increase domestic energy supply, the Japanese government plans for 22–24% of electricity to be generated by renewables in 2030 [4]. Work is in progress to set up a marine energy test centre, similar to the European Marine Energy Centre in Scotland, in the Goto Islands of Nagasaki Prefecture [5].

* Corresponding author.
E-mail address: simon@simonwaldman.me.uk (S. Waldman).

https://doi.org/10.1016/j.ijome.2017.09.002
2214-1669/

1.2. Geographic & hydrodynamic situation

The Goto Islands are an archipelago approximately 80 km to the west of Nagasaki city and, at their closest point, separated from the Japanese mainland by approximately 20 km of sea (Fig. 1a). To the north is the Korea Strait, the main southern entrance to the Sea of Japan, while to the south lies part of the East China Sea and the Pacific Ocean. A portion of flow between these large bodies of water must pass through or around the archipelago.

Within the islands there are four channels running from north-west to south-east, three of which are approximately parallel and of similar dimensions: 7–8 km in length, 1–3 km in width, and 50–60 m deep in mid-channel. These are the Tanoura, Naru and Takigawara Straits (Fig. 1b). The first two have been designated by the Japanese government as an area for tidal energy development, and the first tidal energy convertor (TEC) is due to be installed by OpenHydro in the Naru Strait in 2018 [6]. The fourth channel, the Wakamatsu Strait, is less than 30 m deep for most of its length and is hence unsuitable for the TEC design considered here.

The region experiences mixed diurnal/ semi-diurnal tides. When compared to European seas, less of the energy is to be found in the M2 constituent and a greater proportion (approx. 15% of the total) is in K1 and O1. Table 1 shows the most important constituents.

1.3. Theoretical background & prior work

To extract tidal stream (or "hydrokinetic") energy, a porous obstruction is placed in the flow in the form of a TEC. A proportion of the kinetic energy passing through the TEC is removed for conversion to electricity and a retarding force is applied to the flow, usually resulting in a reduction in its speed. For a given array in a given channel a there exists an optimum proportion of energy removed, beyond which the flow is retarded to such an extent that the available power diminishes.

Garrett and Cummins [8] described a theoretical model of a channel between two large bodies of water, and used this to derive an approximate formula for the power lost to a channel as a result of energy extraction at optimum yield. Their model assumes that the extraction of energy in the channel cannot influence the elevation difference across the channel, which may be thought of as the "head" available to the turbines.

The exportable power available from the turbines cannot exceed the power extracted from the flow, and will usually be less. Losses include drag from the TECs' supporting structures, turbulence generated at the turbine blades, and inefficiencies in the conversion to electrical energy. Where the array does not fill the cross-section of a channel, some flow will divert around it. The kinetic energy of this bypass flow is clearly not available for conversion, but some of it will still be lost from the channel in turbulent mixing when the bypass flow meets the slower wake behind the turbine [9]. Thus, so long as financial limitations on the number of turbines do not apply, a tidal stream array occupying the entire cross-section of a channel will always be optimal. This was demonstrated with theoretical models by Garrett and Cummins [10] and Houlsby et al. [11].

The behaviour of multiple channels has been studied from a theoretical perspective by Atwater and Lawrence [12], who considered the available power in terms of head loss, and Cummins [13], who used the analogy of an electrical circuit.

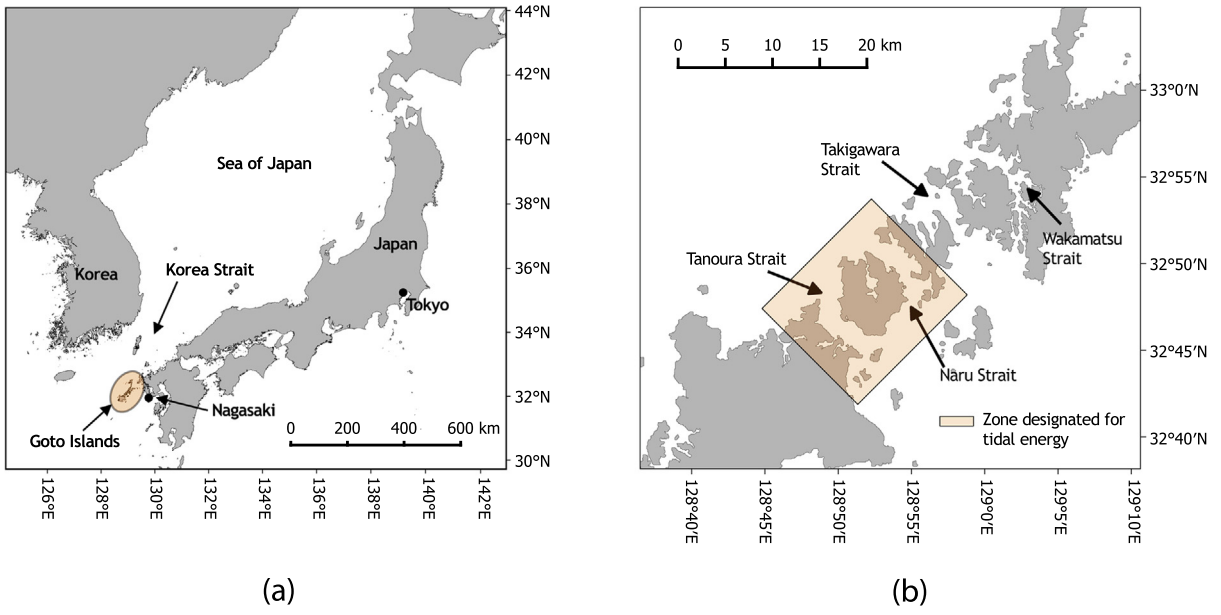

Fig. 1. Maps showing (a) the situation of the Goto Islands with respect to Japan, and (b) the four channels running through the middle of the archipelago.

Table 1
Table showing the five most energetic tidal constituents, based on a 29 day time series of surface elevation from a combined pressure sensor and ADCP deployment in the Naru Strait [7]. Harmonic analysis conducted using the U-Tide software.

Constituent	Proportion of total energy (%)
M2	65.2
S2	13.2
K1	9.2
O1	6.0
N2	2.7

Practical modelling investigations of the multiple channels in the Pentland Firth, Scotland, have been conducted by Draper et al. [14] (in two dimensions), Goward Brown et al. [15] (in three dimensions), and O'Hara Murray and Gallego [16] (in three dimensions, with the same software used here). In all of these studies, where there are parallel sub-channels, there is a tendency for exploitation of one channel to cause flow to be diverted into unexploited sub-channels, reducing the yield.

The authors are unaware of any prior resource assessments of the Goto Islands that account for the effects of energy extraction, and hence the estimates offered by this paper may be the first available.

1.4. Outline of this paper

The work described in this paper has two goals: Firstly, to provide an initial tidal resource assessment for the Goto Islands, and secondly to explore the behavior of the parallel channels when energy is extracted.

Section 2 describes the numerical model that was used. Sections 3–5 relate simulations using realistic TEC representations, aimed at estimating the available resource. In Section 6 we put aside the realistic TEC parameters in an effort to explore the maximum possible extractable power in one of the channels and its effect on the other straits. Section 7 discusses our findings and compares the behavior of the Goto Islands to that of the well-studied Pentland Firth.

2. Description of the model

Numerical simulations were conducted using the free surface three-dimensional Finite Volume Community Ocean Model (FVCOM) [17]. The model used in this work was developed by others at Kyushu University in collaboration with the second author. It will be summarised here, but is described more fully in [7].

The computational domain, shown in Fig. 2, consists of non-overlapping unstructured triangular mesh elements (Fig. 3). The use of an unstructured mesh is efficient in allowing coverage of a large area with fine scale detail in areas of interest. A typical element size of 50 m was adopted around the three narrow channels in the Goto Islands, gradually increasing to 5000 m toward the open boundary. Vertical discretization is provided by 20 equally-spaced sigma layers.

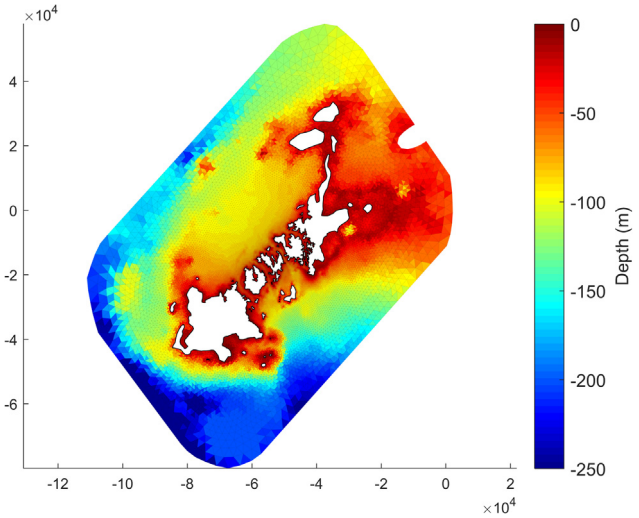

Fig. 2. Plot showing the model domain and bathymetry. The spatial coordinates are in metres, referring to the "Japan Plane Rectangular" coordinate system zone CS1, EPSG ref 2443.

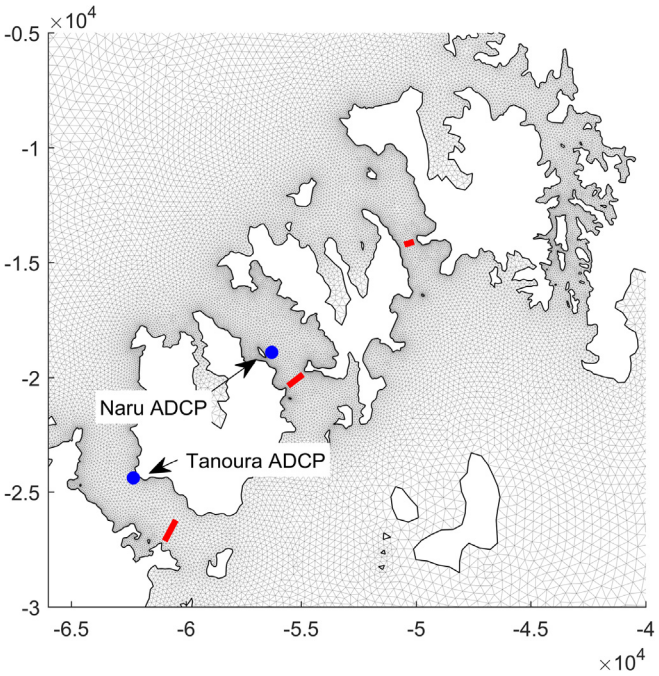

Fig. 3. Plot showing the inner part of the computational mesh. Thick red lines show the locations used for tidal turbines, as described in Section 3. Blue points show the locations of ADCP surveys used for validation. Spatial coordinates are in metres, referring to the "Japan Plane Rectangular" coordinate system zone CS1, EPSG ref 2443.

The horizontal velocity components (u, v) are calculated at the centroid of each triangle while elevations are calculated at the vertices. FVCOM is closed mathematically using a modified Mellor and Yamada level 2.5 turbulence closure scheme [18] for vertical eddy mixing and the Smagorinsky parameterization [19] for horizontal eddy viscosity.

The model bathymetry (Fig. 2) was produced from data supplied by the Hydrographic and Oceanographic Department, Japan Coast Guard. Eight major tidal constituents (M2, S2, K2, N2, K1, O1, P1, Q1) were forced at open boundary nodes using amplitudes and phases based on the NAO.99Jb regional tide model [20]. The phases of these forcing constituents were then adjusted as part of the calibration procedure to improve the agreement with measurements in the tidal straits. The model was run in barotropic mode with no freshwater inputs or meteorological effects.

The model was validated by comparison of velocities at two locations (see Fig. 3) between ADCP measurements and model predictions over a two-week period. Error and correlation statistics are reproduced in Table 2 and show an excellent match in the Tanoura strait. In the Naru strait the correlation is poorer for the u-velocity, but since the flow in this location is dominated by the north–south axis this was considered acceptable. A harmonic analysis of surface elevation at a tide gauge station was also conducted, and the comparison between these measurements and predictions is shown graphically in Fig. 4.

2.1. Energy extraction

The code used to represent energy extraction was that of O'Hara Murray and Gallego [16], which follows the approach of Yang et al. [21] and incorporates tidal stream energy extraction into FVCOM using a sub-grid scale momentum sink method. This approach represents the horizontal retarding force, applied by tidal stream turbines on the flow, as additional terms in the 3D momentum equations. The retarding force can be applied at any vertical layer, or combination of layers. Assuming a tidal turbine is always orientated to face the current, *i.e.* it weathervanes to face the flow, the retarding force can be expressed as a quadratic drag law

$$F = \frac{1}{2}\rho C_T A|\mathbf{u}|\mathbf{u} \tag{1}$$

Table 2
Table showing RMSE and R^2 statistics for comparison of depth-averaged velocities between observations and predictions at two locations (see map in Fig. 3).

Location	u-Velocity		v-Velocity	
	RMSE (ms^{-1})	R^2	RMSE (ms^{-1})	R^2
Tanoura Strait	0.18	0.94	0.31	0.92
Naru Strait	0.26	0.79	0.24	0.93

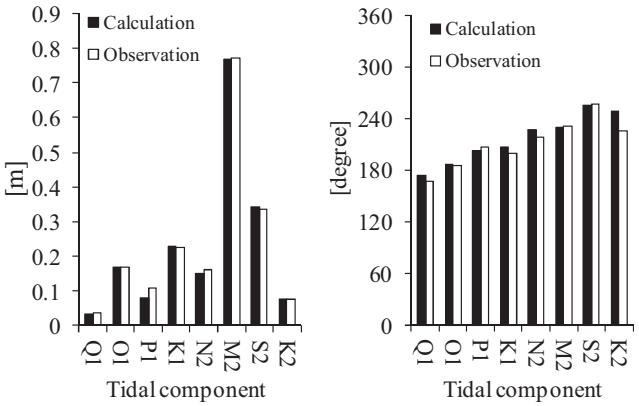

Fig. 4. Chart comparing predicted and observed amplitudes (left) and phases (right) of eight tidal constituents at the location of a tide gauge in Fukue City. This location is a short distance beyond the southern edge of Fig. 3, at 32.7°N, 128.85°E. Note that phases at the open boundaries were adjusted during calibration.

where ρ is the water density, C_T is the thrust coefficient of the turbine, A is the flow facing area of the turbine, and $\mathbf{u}$ is the flow velocity vector. For simplicity, no supporting structures were included in the model.

FVCOM uses a mode splitting method in order to solve the 2D, depth averaged, barotropic equations, and the 3D baroclinic equations, with different time steps [17]. Therefore, additional terms were added to both the 2D and 3D momentum equations. In order to allow for the turbines to span multiple vertical layers a parameter K, expressing the fraction of A occupied by the turbine in each layer was included. Thus, equations for the retarding force exerted by N turbines on the fluid for any model element, i, and for the 2D and 3D equations respectively, are

$$F_{2D}(i) = \frac{1}{2}\rho N(i) C_T(i) A(i) \sum_{j=1}^{n} K(i,j) |\mathbf{u}(i,j)| \mathbf{u}(i,j) \tag{2}$$

$$F_{3D}(i,j) = \frac{1}{2}\rho N(i) C_T(i) A(i) K(i,j) |\mathbf{u}(i,j)| \mathbf{u}(i,j) \tag{3}$$

where j is the depth layer, and n is the total number of depth layers. $N(i)$, $C_T(i)$, $A(i)$,and $K(i,j)$ can all potentially vary between mesh elements, *i.e.* depending on the water depth and the number and type of turbines deployed in each element. $C_T(i)$ may be expressed as a function of $u(i)$ using a lookup table and linear interpolation, to allow for the representation of realistic thrust curves. A full description of the energy extraction implementation can be found in [16].

The simulated TEC was based on the OpenHydro device that has been proposed for the Naru Strait. This is a seabed-mounted design with a diameter of 16 m, a hub height of 19 m above the seabed, and a rated capacity of 2 MW (OpenHydro, personal communication with SY). A realistic thrust curve was applied, based on that given by Baston et al. [22] but scaled to use a cut-in speed of 1 ms^{-1} and a rated speed of 3 ms^{-1}. This rated speed was adopted because it is a speed that is regularly encountered during spring tides in the area of interest; the turbine's rated capacity of 2 MW would imply a rated speed of over 3.5 ms^{-1}, but it is unlikely that this would ever be reached. The thrust coefficient between the cut-in and rated speeds is 0.85, while above the rated speed it is scaled to provide a constant power output.

Two limitations of the current implementation of energy extraction are the assumption that TECs always face the flow (which is unlikely to be the case with the OpenHydro design, which does not yaw) and the definition of the vertical position of the momentum sink in terms of sigma layers, causing the simulated TECs to move up and down with the rise and fall of the tide.

2.2. Calculation of power

Electrical power was calculated from simulated current speeds as a post-processing step. Initially, thrust was determined using (1). Power was then estimated using

$$P = C_C F |\mathbf{u}| \tag{4}$$

where C_C is a coefficient that represents the conversion losses between kinetic energy in the flow and electricity. It is acknowledged that some inaccuracy is inherent in using the same value of $|\mathbf{u}|$, representing an entire mesh element, in both of the equations above (more correctly, the velocity in (1) should be the free-stream velocity and that in (4) should be the velocity at the turbine, but neither of these values is known to the model), and correction for this is implicitly included in the value of C_C. A value of 0.5 was assigned to C_C based on experimental results with a Schottel turbine reported by Jeffcoate

et al. [23]. This two-stage approach is equivalent, below the rated speed, to a power coefficient of 0.425, which is within the range shown by Bahaj et al. [24] from tank testing.

3. Single-channel scenarios

A transect across each strait between the 30 m depth contours was identified to hold TECs. This depth limitation allowed for the full height of the TEC (27 m from base to blade tip) to remain submerged throughout the tidal cycle. Simulated turbines were placed, evenly spaced, along these lines, and the number of turbines lying inside each intersected mesh element was provided to the FVCOM model. The transects were located by inspection of the areas of highest speeds without turbines on both flood and ebb, which were usually at or near to the narrowest parts of the channels. Their locations can be seen in Fig. 3.

A wide range of turbine numbers was tested in each channel, from the conservative to the implausible. In the more heavily exploited scenarios a single row of turbines is unrealistic, as they would be placed very close together and even overlap and collide. However, this approach allowed the level of energy extraction in a channel to be reduced to a single parameter, which is convenient and, in the event of performing an optimisation across multiple channels, reduces the number of degrees of freedom. Since the purpose of this work was not to study realistic array layouts but to examine the behaviour of the channel as a whole, this was judged to be acceptable.

In order to minimise computation time, initial simulations were driven only by the M2 tidal constituent. This allows the use of just 12.4 h of output – a single M2 cycle – as a representative time period. It was determined empirically that the model required 3 days of spinup time before its output became fully periodic, so each scenario was run for 4 days of model time and the output data taken from the final 12.4 h.

Fig. 5 shows the maximum and mean power output for each channel with scenarios between 5 and 1000 turbines. The use of M2 only means that results in this section show unrealistically low levels of power, so limited attention should be paid to the absolute power levels; of interest instead are the differences in output between different scenarios. It is clear that even with modest numbers of TECs, additional machines offer diminishing returns. The mean power available in each strait peaks at implausibly high levels of exploitation, ranging from 270 to 446 TECs; beyond this point, adding additional turbines gives a negative marginal return. The maximum power also peaks in each channel, but at even higher numbers of TECs than the mean.

O'Hara Murray and Gallego [16] noted that when simulating turbines in their correct vertical locations, as done here, a portion of the flow would divert over and under the turbine rotors instead of passing through them (although in reality, or in a more detailed simulation, some of the flow under the rotor would be impeded by the device's base structure). This behavior appears to be replicated in the Goto channels, as suggested by Fig. 6. Vertical diversion limits the power output that can be achieved, but is unavoidable while using bottom-mounted turbines and while, in some areas, preserving clear water above for navigation.

The use of realistic TEC arrangements will be continued for the next two sections to arrive at realistic resource estimates. In Section 6 the TEC description will be modified to explore the maximum power that can be extracted without engineering or navigational constraints.

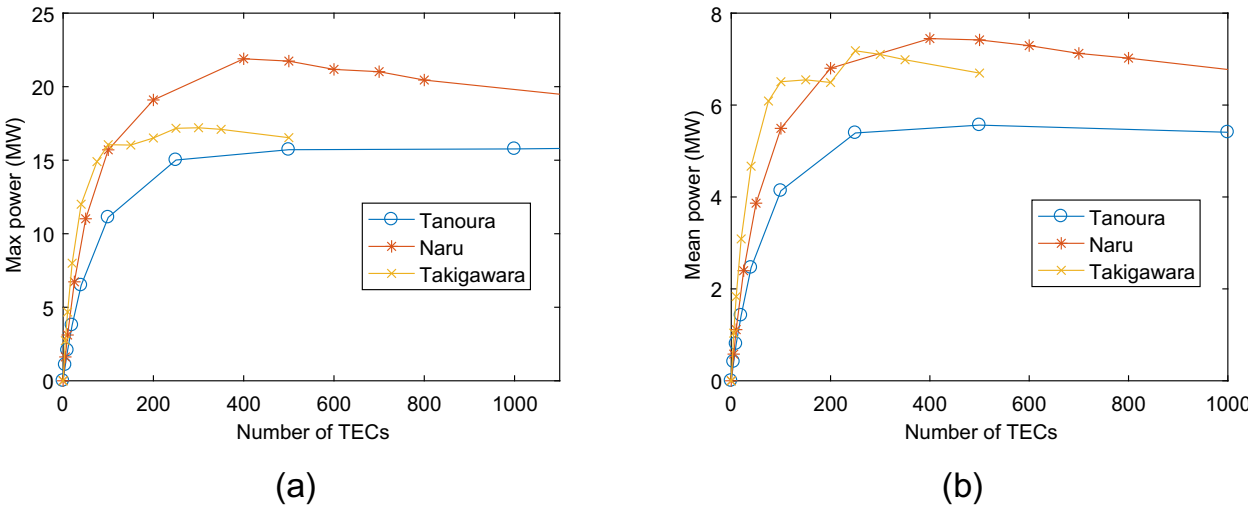

Fig. 5. Plots showing (a) maximum and (b) mean power output from the three channels with varying numbers of realistic TECs. The maximum power in the Tanoura strait peaks at approximately 2400 TECs, beyond the limits of this plot.

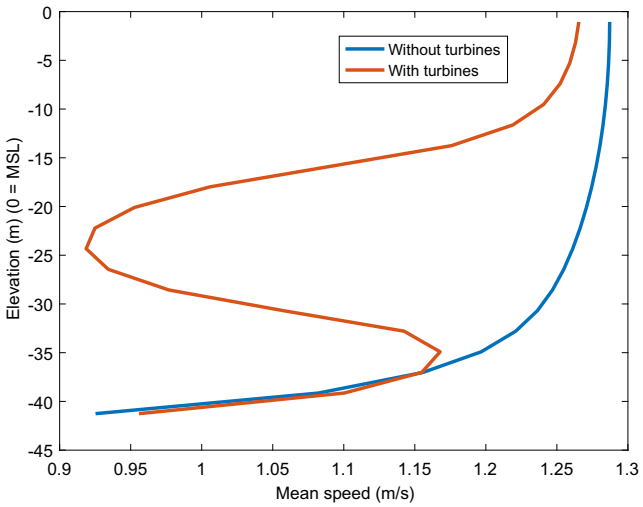

Fig. 6. Vertical speed profiles showing mean current speed over 24 h with and without TECs. The scenario used for "with turbines" is that of 100 TECs in the Naru strait, and the mesh element used is that with the greatest number of TECs in this scenario.

4. Interactions between channels

Fig. 7 shows the effect on mean depth-averaged current speeds of placing 100 TECs in the Naru Strait. A reduction in mean speed of up to 0.15 ms^{-1} through the TECs is seen, as expected, and an increase of 0.1 ms^{-1} occurs at the sides of the channel around the array. Adding impedance to the Naru Strait has only small effects on the other channels; mean speeds in the Tanoura Strait are affected by less than 0.02 ms^{-1}, and those in the Takigawara Strait by slightly more.

There are substantial areas of change to the north and south of the islands. These appear to be caused by changes in the positions of eddy structures that form at the downstream ends of the channels.

The equivalent maps for the other two channels are not shown, but the qualitative results are similar: reductions in mean speed in the exploited channel, but only small changes in other channels.

In order to provide a quantitative perspective on inter-channel effects a series of simulations was conducted, using only the M2 constituent, with 60 TECs in each channel and in each combination of channels. Comparisons were made between the maximum and mean power outputs of these channels, and in particular between the power provided by a scenario with two

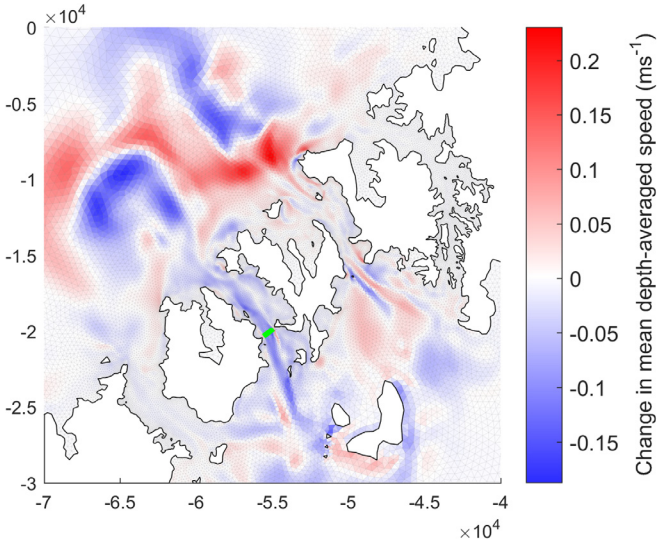

Fig. 7. Map showing the change in mean current speed over an M2 cycle in each mesh element as a result of adding 100 TECs to the Naru Strait. Green line shows location of turbines. Spatial coordinates are in metres in the "Japan Plane Rectangular" coordinate system zone CS1, EPSG ref 2443.

Table 3
Table showing mean and maximum outputs from different combinations of channels. 60 turbines were used in the exploited channels. Sums are on a per-timestep basis. The models were forced with M2 only, so the power estimates will be unrealistically low.

Channels exploited	Mean power (MW)	Max power (MW)
Tanoura alone	3.2	8.4
Naru alone	4.3	12.3
Takigawara alone	5.6	13.8
Sum of Tanoura & Naru separately	7.4	20.3
Tanoura & Naru together	7.5	20.5
Sum of Naru & Takigawara separately	9.9	25.2
Naru & Takigawara together	10.0	25.2
Sum of all 3 separately	13.1	32.7
All 3 together	13.2	32.3

or three channels together and the sum of the powers provided by each of those channels alone; interactions between the channels would result in differences between these values.

The results of these simulations are shown in Table 3, and show an increase in mean power of the order of 1% from using two channels together, indicating that some interaction does exist but that it is weak. The reason that "all 3 together" has a lower maximum power, but a higher mean power, than the sum of 3 separately, is unclear. It may relate to slight phase differences in the progress of the tide through the channels.

The low level of interaction between channels in Goto contrasts with the findings of Draper et al. [14] in the Pentland Firth, where the power available in each subchannel depended markedly upon the level of exploitation in the others.

5. Estimating the resource

Thus far simulations have been driven only by the M2 constituent in order to minimise computation time. However, only 65% of tidal energy in this region is in M2 (see Table 1), and so this does not give a useful estimate of the available power.

Four "candidate scenarios" were identified to be run for 28 days (plus spinup) with eight constituents. Three corresponded to low, medium and high levels of development, where for each scenario the turbines of each channel had the same capacity factor. This was intended to represent a similar level of return on investment in each channel. The actual values of the capacity factors are not meaningful due to both the unrealistic array layouts and the use of M2 only, and so are not reported here. In the fourth scenario, termed "optimum", each channel had the number of turbines that corresponded to the greatest mean power output attainable over an M2 cycle. This "optimum" number of TECs may be different with more constituents than with M2 only, and indeed may change with improved array layouts, but the number established here is used as an approximation that is available while keeping computing times low. The optimum number of TECs was calculated using simple parabolic interpolation between the highest-power scenario in Section 3 and the two either side of it.

It should be noted that this approach, where each channel is optimised independently and then the indicated level of deployment for each combined in a single model, is not generally applicable; it is appropriate in situations such as this one where the channels do not interact significantly with one another, and avoids the need for a more difficult simultaneous optimisation of all channels.

Each of the four scenarios was simulated with all three channels active and with turbines in the Takigawara Strait removed, thus including only the channels currently designated for development. Table 4 shows the mean and maximum power outputs of each scenario, as well as the ratio of mean to maximum power output.

Table 4
Table showing the number of turbines allocated to each channel in each scenario, and the predicted power outputs. Scenarios marked "A" use only the two channels designated for tidal development, while those marked "B" use all three.

Level of development	Number of turbines				Power (MW)		Mean/Max
	Tanoura	Naru	Takigawara	Total	Mean	Max	
Low (A)	5	42	0	47	4.70	23.50	20%
Medium (A)	46	88	0	134	9.67	48.38	20%
High (A)	130	190	0	320	14.08	69.01	20%
Optimum (A)	414	446	0	860	16.25	79.30	20%
Low (B)	5	42	73	120	11.93	49.49	24%
Medium (B)	46	88	112	246	17.73	75.16	24%
High (B)	130	190	182	502	22.34	97.35	23%
Optimum (B)	414	446	270	1130	24.53	106.78	23%

It is notable that at low levels of exploitation, the Takigawara Strait is predicted to give the most power at a given capacity factor, offering more than the other two channels combined in the "Low" scenario. At higher levels of development the Naru strait has more potential, matching the M2-only predictions in Fig. 5. In all scenarios, the ratio of mean:max power is higher when the Takigawara Strait is included than when it is not.

6. Exploring the maximum power in the Naru Strait

In earlier sections a realistic representation of a bottom-mounted TEC was used. As noted in Section 3, this only occupies a portion of the water column and allows the flow to divert over and under the rotor. Additionally, the limitation of not placing TECs in water shallower than 30 m allows large regions of horizontal diversion in some channels. In this section these restrictions are discarded in an effort to maximise the energy available in one channel – the Naru Strait – and look for any response in the other channels.

Three changes were made from earlier scenarios:

1. Instead of extracting momentum from the vertical layers intersected by the rotor, the same thrust was applied evenly across all layers. This simulates the way that energy extraction would appear in a two-dimensional model, and approximates a possible future scenario where a large number of smaller TECs, with lower individual thrust, are deployed at different depths throughout the water column. Such a deployment might be possible through designs such as the Triton device [25] that is planned for deployment in the Bay of Fundy. The same approach of "smearing" thrust throughout the water column was used by O'Hara Murray and Gallego [16] for some scenarios in their modelling of the Pentland Firth.
2. Instead of placing turbines along a line between the 30 m contours, the line was extended to run from coast to coast. This is unrealistic with a natural coastline, but could be achieved through civil engineering works to provide a minimum depth.
3. The thrust curve, previously a function of the current speed, was changed to a constant value of $C_T = 0.85$. This is because the presence of a cut-in speed would otherwise set a limit on how far the TECs could reduce the transport through the channel. This constant thrust coefficient is probably unrealistic, but it is certainly possible that future TECs will have cut-in speeds below the 1 ms^{-1} that was used to this point.

The M2-only simulations of the Naru Strait were repeated with these modifications. Additionally, transport through the northern mouth of the strait was recorded for each scenario. This was calculated by taking 200 sample points along a straight line from coast to coast, extracting mean depths and depth-averaged velocities normal to this line at each point, and using simple trapezoidal integration. The number of TECs was increased far beyond commercially realistic levels until a maximum power output was found past which the marginal change in power for extra TECs was negative. Fig. 8 shows the power output as a function of the number of turbines, and Fig. 9 relates it to the reduction in transport through the channel.

The maximum power available from the Naru Strait (M2 only) under these artificial conditions is predicted as approximately 36 MW, with between 600 and 800 turbines. This maximum occurs when transport through the channel is reduced by 36%; additional impedance, and further reductions in transport, beyond this point result in decreased power output.

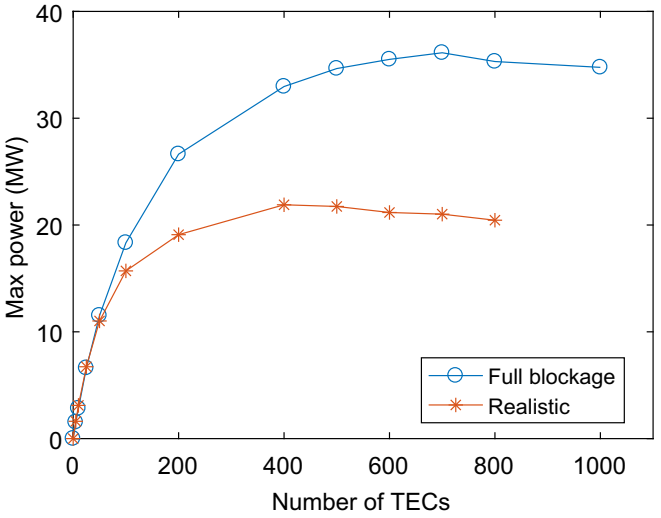

Fig. 8. Maximum output during a tidal cycle from M2 only with turbines evenly spread across full channel height and width, with no cut-in speed, compared to the realistic circumstances of Section 3.

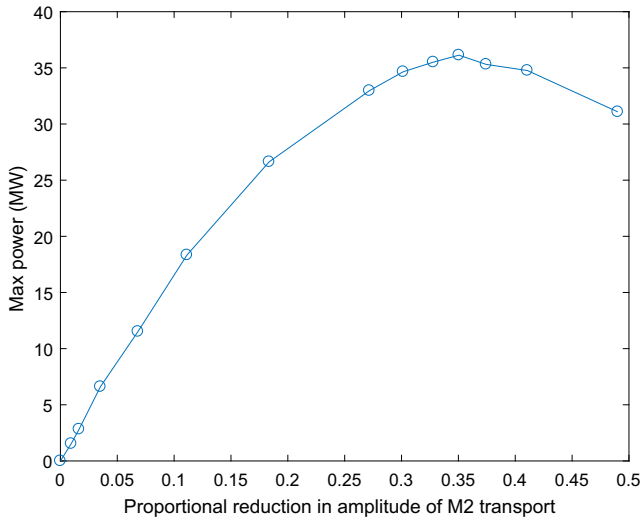

Fig. 9. Maximum power output during a tidal cycle from M2 only with turbines evenly spread across full channel height and width, with no cut-in speed, plotted against proportional reduction in the maximum transport.

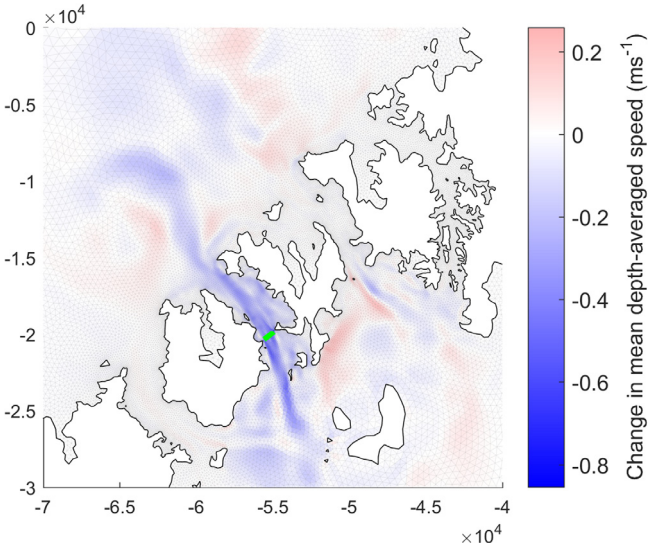

Fig. 10. Map showing the change in mean current speed over an M2 cycle in each mesh element as a result of adding 700 TECs to the Naru Strait, covering the full cross-section of the channel. Green line shows the location of turbines. Spatial coordinates are in metres in the "Japan Plane Rectangular" coordinate system zone CS1, EPSG ref 2443.

Fig. 10 shows the effect on mean current speeds of 700 turbines across the full height and width of the Naru Strait. The effects in the exploited strait are unsurprisingly much greater than those with 100 turbines in Fig. 7. Once again, it is clear that there is minimal effect on the other channels through the archipelago.

7. Discussion

7.1. Capacity of Naru Strait

When pushing the simulated Naru Strait to its limit of available power, through unrealistic array layouts and turbine parameters, maximum power (36 MW) was predicted with a reduction in transport through the channel of 36%. This may be compared against similar values found in modelling the Pentland Firth of 38% [16] and 42% [14], and is within the range of 29–42% that is given from theory by Garrett and Cummins [8].

The maximum power that can be removed from this channel can be compared to that predicted by the Garrett & Cummins model:

$$P_{lost} = \gamma \rho g a Q_{\max} \tag{5}$$

where γ is set to 0.20 based on a phase lag between head and transport, measured from the model, of 24°. Using values for $Q_{\max}$ and a from the model, this predicts a maximum power of 65 MW.

Garrett and Cummins noted that an assumption in their model was that there was no "back effect", *i.e.* the height difference between the ends of the channel is not increased by the imposition of the turbines. As shown in Fig. 11, there is a small but noticeable back effect in the case of the Naru Strait at optimal yield, which should cause an increase in both flow and yield. Our calculation of power includes an efficiency factor of 0.5 in (4), and once this is taken into account our value of 36 MW is indeed slightly greater than that suggested by the simple model. We find the level of agreement between these values encouraging.

Comparison with the realistic turbine setup used in earlier sections (Fig. 8) shows, as mentioned with respect to theory in Section 1.3, that spreading a given thrust evenly across a channel will maximise the available power. While this is difficult to realise with bottom-mounted TECs, and while allowing room for navigation, it is possible to design tidal energy projects to get as close to this ideal as possible given the available technology and constraints. It is likely that some of the benefit of filling the channel cross-section with TECs could be realised by using a lesser quantity of TECs and reducing the channel cross-section, or increasing the impedance of bypass areas, with passive civil engineering measures. However, we have not modelled this option and it may have severe environmental impacts.

The difference between the realistic and non-realistic scenarios, in terms of the vertical distribution of thrust, highlights the importance of using three-dimensional models for resource assessment work – a conclusion also reached by Goward Brown et al. [15].

7.2. Interaction between channels

In the Pentland Firth, Scotland, Draper et al. [14] found strong connections between subchannels; exploiting one led to flow diversion into others, and exploiting all together gave more power than the sum of each channel alone. This does not appear to be the case in the Goto Islands. While in some respects the channel systems of the Goto Islands and the Pentland Firth are quite similar, there are notable differences in the connectivity between their channels.

Both the Pentland Firth and the Goto channels run between large bodies of water that are strongly connected by other routes, and hence whose surface elevations cannot be altered by changes to the transport through the channels in question (although local changes around the channel mouth(s) are possible). Thus the head over the archipelago as a whole is approximately fixed, but the distribution of the head loss within the isles may be altered by the addition of TECs.

In the Pentland Firth, the three sub-channels merge at either end into a single main channel. If a single channel is exploited, then (assuming low impedance in unexploited channels) the maximum head available for generation is slightly greater than the undisturbed elevation change over the length of the divided subchannel. This is because once the head reaches this level it also affects the other subchannels and causes flow to divert into them, resulting in the strong interactions that are predicted in that region. The full potential of the elevation difference between the Atlantic and the North Sea is thus only available if all three subchannels are exploited together.

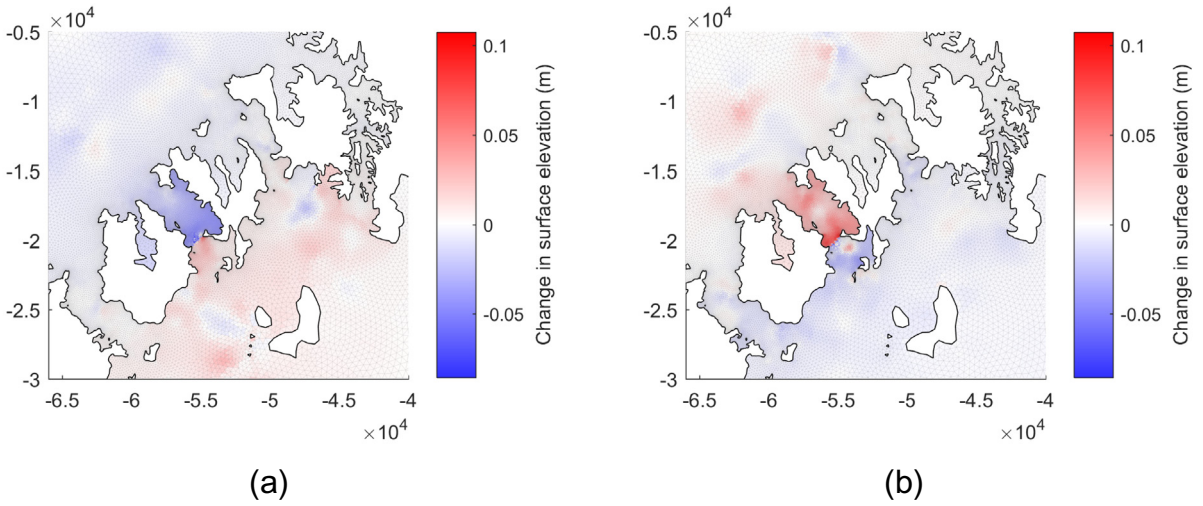

Fig. 11. Maps showing the change in surface elevations at single timesteps during (a) flood and (b) ebb, as a result of adding 700 turbines to the Naru Strait with full horizontal and vertical blockage.

In Goto, by contrast, the three main channels are almost entirely distinct, opening directly into the large bodies of water that they link without an intervening combined channel. As a result the full potential drop across the islands is available for energy extraction in any or all of the channels independently. Because there is no combined channel, and because the channel mouths are separated by significant distances, local elevation changes at one channel mouth are greatly diminished before they reach other channels. This results in very weak interactions between the straits.

Fig. 11 shows the changes in surface elevations as a result of adding 700 turbines to the Naru Strait. It is clear that the elevation gradient of that channel is dramatically altered – with water level upstream of the TECs increased and that downstream decreased, and most of the potential drop concentrated on the line of turbines. This effect does propagate weakly beyond the ends of the channel, in particular to the south, and this is probably because the bay-like shape of the archipelago here acts as a buffer between the Naru Strait and the South China Sea. However, this wider effect is small (generally < 1 cm) and there is almost no change in the elevation drop across the other straits.

While there seems to be a satisfactory explanation for the behaviors of the two locations mentioned here, it would be beneficial to establish a more general description of the interactions of parallel channels.

7.3. Resource estimation

Estimating resource in the channels of Goto is more straightforward than in some areas because the channels do not significantly affect one another. In other areas it would be necessary to perform a difficult optimisation with at least as many degrees of freedom as there are channels, but in Goto one can simply arrive at a resource estimate for each channel and sum them.

In this case the number of turbines required to obtain the greatest possible mean output from each channel is very high, and unlikely to be commercially viable. Therefore, in addition to optimising for mean power, we have selected three arbitrary scenarios which have equal capacity factors (CF) in each channel. These scenarios were each run for 28 days with eight tidal constituents, and we report a maximum (peak) and mean (time-averaged) power for each scenario. The total available power from the three channels reaches maxima of 49.5, 75.2, and 97.4 MW at low, medium and high levels of exploitation respectively. The mean power in each scenario is consistently 23–24% of the maximum. There is a greater difference between mean and maximum here than is common in European waters, which may make development slightly less economically attractive. The relatively high variation in this study area can be attributed to its mixed diurnal and semidiurnal tides.

The maximum available resource in just the Tanoura and Naru straits, which are those designated for tidal energy development, is 23.5, 48.4, or 69.0 MW for the three scenarios. It is interesting to note that the channel with the greatest output in the low deployment scenario (probably the most economically attractive scenario) is the Takigawara Strait, which is not within the designated development area. Omitting the Takigawara Strait also reduces the Mean:Max power ratio to 20%.

The Wakamatsu Strait has been excluded from this study due to its shallow depth. However, future generations of TEC design may be able to operate in a wider range of speeds and water depths [26], and hence may open this additional channel to exploitation as well as increasing the power available from the other straits due to lower cut-in speeds.

The relatively modest capacities of these channels means that, even at quite low levels of development, TECs' performances within any single channel will not be independent of one another. This will have implications for the management of the planned marine energy test centre, where a number of device developers might be testing different technologies within the same channel and may be affected by each others' activities.

8. Conclusions

In this work, numerical modelling has been used to predict the effects of tidal energy extraction from the Tanoura, Naru and Takigawara Straits in the Goto Islands using tidal energy converters (TECs) of the type planned by OpenHydro for deployment in the region. We estimate that between 24 and 79 MW of power is available, depending on the level of development, from the designated tidal energy zone, and that between 50 and 107 MW is available from all three channels together, using the currently proposed bottom-mounted turbines (Table 4). We note that the channel with the greatest potential at early stages of development (the Takigawara Strait) is not in the designated area.

As the level of energy extraction increases the marginal gain from adding additional turbines decreases, both because of a reduction in transport through the channel as a result of the increased impedance and because flow tends to divert over and under the rotors. TECs occupying more of the water column can use the same total rotor area more efficiently, which may be achievable in future using a larger number of smaller rotors.

Because modest levels of exploitation have noticeable effects on transport, managers and clients of the planned tidal energy test centre will need to be aware that the performance of a given device or array may be influenced by other test activities occurring in the same channel.

The maximum power that could, in principle, be generated from the Naru strait from M2 only is estimated to be 36 MW, in contrast with 22 MW using realistic technology. The necessary conditions for this higher output are unrealistic and undoubtedly uneconomical, but it is possible that civil engineering works to modify the channel, together with different designs of TEC, could permit a closer approach to this maximum. We have not studied the environmental consequences of such works.

There is little interaction between the channels in the Goto Islands, meaning that any or all of them can be exploited independently of the others. This may increase the attractiveness of the area for development, as – unlike Scotland's Pentland Firth – it is not necessary to develop all channels to realise the full potential of one. The interaction of parallel channels is sensitive to their geometry, and it would be useful to understand this more fully.

Acknowledgements

This work was made possible by a research exchange to Kyushu University, Japan. Travel funding was received from the MASTS pooling initiative (the Marine Alliance for Science and Technology for Scotland) and their support is gratefully acknowledged. MASTS is funded by the Scottish Funding Council (grant reference HR09011) and contributing institutions. We thank Kyushu University, and in particular Prof. Changhong Hu, for hosting the exchange and providing office space and computing time. The participation of David Woolf was enabled by the UK Engineering and Physical Sciences Research Council (EPSRC) through the EcoWatt2050 project (EP/K012851/1). The Ministry of Environment of Japan is gratefully acknowledged for permission to use observation data, which were obtained through the project for "Promotion of Realization of Tidal Current Power Generation", supported by the Ministry, in 2014 and 2015. The FVCOM model of the Goto Islands was originally developed and validated by Dr. Huihui Sun, and FVCOM itself is by Dr. Changsheng Chen. The first author thanks Dr. Patxi Novo Garcia for both technical assistance and friendship during his time in Japan.

References

[1] Statistics Japan, Japan Statistical Yearbook 2015, Table 11–14 "Electrical power generated", http://www.stat.go.jp/english/data/nenkan/65nenkan/1431-11.htm, accessed 2016-11-07, 2016.
[2] US Energy Information Administration, Japan: International energy data and analysis, https://www.eia.gov/beta/international/analysisincludes/countrieslong/Japan/japan.Pdf, accessed 2016-11-07, 2015.
[3] J.D. Bricker, M. Esteban, H. Takagi, V. Roeber, Economic feasibility of tidal stream and wave power in post-Fukushima Japan, Renewable Energy, ISSN 0960-1481. doi:https://doi.org/10.1016/j.renene.2016.06.049.
[4] World Nuclear Association, Nuclear Power in Japan, http://www.world-nuclear.org/information-library/country-profiles/countries-g-n/japan-nuclear-power.aspx, accessed 2016-11-07, 2016.
[5] M. Iwata, Nagasaki plans asia first major testing site for marine energy, Wall Street J. http://blogs.wsj.com/japanrealtime/2015/04/01/nagasaki-plans-asias-first-major-testing-site-for-marine-energy/, accessed 2016-11-07.
[6] OpenHydro, OpenHydro secures Japanese tidal turbine contract (press release), http://www.openhydro.com/OpenHydro/media/Documents/News accessed 2016-11-17, 2016.
[7] H. Sun, Y. Kyozuka, T. Yamashiro, Tidal current power potential in Goto Islands by observations and simulations, in: 2nd Asian Wave & Tidal Energy Conference (AWTEC), Tokyo, 2014.
[8] C. Garrett, P. Cummins, The power potential of tidal currents in channels, Proc. R. Soc. A: Math. Phys. Eng. Sci. 461 (2060) (2005) 2563–2572, https://doi.org/10.1098/rspa.2005.1494.
[9] R. Vennell, The energetics of large tidal turbine arrays, Renewable Energy 48 (2012) 210–219, https://doi.org/10.1016/j.renene.2012.04.018, 210–219, ISSN 09601481.
[10] C. Garrett, P. Cummins, The efficiency of a turbine in a tidal channel, J. Fluid Mech. 588, 1469–7645, ISSN 0022-1120. doi:https://doi.org/10.1017/S0022112007007781 .
[11] G.T. Houlsby, S. Draper, M.L.G. Oldfield, Application of linear momentum actuator disc theory to open channel flow, Tech. Rep. OUEL 2296/08, University of Oxford, Oxford, http://www.eng.ox.ac.uk/civil/publications/reports-1/ouel229608.pdf, 2008.
[12] J.F. Atwater, G.A. Lawrence, Power potential of a split tidal channel, Renewable Energy 35 (2) (2010) 329–332, https://doi.org/10.1016/j.renene.2009.06.023, ISSN 0960-1481.
[13] P.F. Cummins, The extractable power from a split tidal channel: an equivalent circuit analysis, Renewable Energy 50 (2013) 395–401, https://doi.org/10.1016/j.renene.2012.07.002, ISSN 0960–1481.
[14] S. Draper, T.A. Adcock, A.G. Borthwick, G.T. Houlsby, Estimate of the tidal stream power resource of the Pentland Firth, Renewable Energy 63 (2014) 650–657, https://doi.org/10.1016/j.renene.2013.10.015, ISSN 09601481.
[15] A.J. Goward Brown, S.P. Neill, M.J. Lewis, Tidal energy extraction in three-dimensional ocean models, Renewable Energy, ISSN 0960-1481. doi: https://doi.org/10.1016/j.renene.2017.04.032.
[16] R. O'Hara Murray, A. Gallego, A modelling study of the tidal stream resource of the Pentland Firth, Scotland, Renewable Energy, ISSN 0960-1481. doi: https://doi.org/10.1016/j.renene.2016.10.053.
[17] C. Chen, H. Liu, R.C. Beardsley, An unstructured grid, finite-volume, three-dimensional, primitive equations ocean model: application to coastal ocean and estuaries, J. Atmos. Oceanic Technol. 20 (1) (2003) 159–186, ISSN 0739-0572, doi: 10.1175/1520-0426(2003) 0200159:AUGFVT2.0.CO;2..
[18] G.L. Mellor, T. Yamada, Development of a turbulence closure model for geophysical fluid problems, Rev. Geophys. 20 (4) (1982) 851–875, https://doi.org/10.1029/RG020i004p00085, ISSN 1944-9208.
[19] J. Smagorinsky, General circulation experiments with the primitive equations, Monthly Weather Rev. 91 (3) (1963) 99–164, ISSN 0027–0644, doi: 10.1175/1520-0493(1963)0910099:GCEWTP2.3.CO;2..
[20] K. Matsumoto, T. Takanezawa, M. Ooe, Ocean tide models developed by assimilating TOPEX, POSEIDON altimeter data into hydrodynamical model: a global model and a regional model around Japan, J. Oceanogr. 56 (5) (2000) 567–581, https://doi.org/10.1023/A:1011157212596, ISSN 0916-8370, 1573-868X.
[21] Z. Yang, T. Wang, A.E. Copping, Modeling tidal stream energy extraction and its effects on transport processes in a tidal channel and bay system using a three-dimensional coastal ocean model, Renewable Energy 50 (2013) 605–613, https://doi.org/10.1016/j.renene.2012.07.024, ISSN 2214-1669.
[22] S. Baston, S. Waldman, J. Side, Modelling energy extraction in tidal flows, revision 3.1, in: TeraWatt Position Papers, MASTS, 75–107, ISBN 978-0-9934256-1-5, http://www.masts.ac.uk/media/166596/positionpapersterawatte-book.pdf, 2015.
[23] P. Jeffcoate, R. Starzmann, B. Elsaesser, S. Scholl, S. Bischoff, Field measurements of a full scale tidal turbine, Int. J. Marine Energy, ISSN 2214-1669. doi: https://doi.org/10.1016/j.ijome.2015.04.002.
[24] A. Bahaj, A. Molland, J. Chaplin, W. Batten, Power and thrust measurements of marine current turbines under various hydrodynamic flow conditions in a cavitation tunnel and a towing tank, Renewable Energy 32 (3) (2007) 407–426, https://doi.org/10.1016/j.renene.2006.01.01, ISSN 09601481.
[25] Black Rock Tidal Power, Technology, http://www.blackrocktidalpower.com/technology/, accessed 2016-11-10, n.d.
[26] M. Lewis, S.P. Neill, P.E. Robins, M.R. Hashemi, Resource assessment for future generations of tidal-stream energy arrays, Energy, ISSN 0360-5442. doi: https://doi.org/10.1016/j.energy.2015.02.038.